



Plasma Prepared Platinum-Carbon Nanotubes as Methanol Oxidation Catalysts for DMFC

Mingming Song,² Qi Wang, Xiao Zuo, and Yuedong Meng

Institute of Plasma Physics, Chinese Academy of Sciences, Hefei, Anhui 230031, China

Ar and H₂ plasma are used to reduce the platinum precursors supported on the O₂ plasma functionalized CNTs. H₂ plasma reduced catalysts with well dispersed nanoparticles and fewer impurities between Pt and CNTs shows an improved catalytic activity in the methanol electro-oxidation and an enhanced tolerance to carbonaceous species.

© 2012 The Electrochemical Society. [DOI: 10.1149/2.020202ss] All rights reserved.

Manuscript submitted April 2, 2012; revised manuscript received May 15, 2012. Published July 20, 2012.

Supported platinum (Pt) nanoparticles have been widely used as catalysts in the direct methanol fuel cell (DMFC).¹ In order to increase the precious metals utilization and improve the catalytic activity, it is generally required that Pt nanoparticles be well dispersed with smaller size, and have strong interaction with supports.² Carbon nanotubes (CNTs) are the most widely used supports due to their unique geometrical, electrical, and mechanical properties.³ However, pristine CNTs have no enough binding sites to anchor the metal precursors because of the high curvature and chemical inertness.⁴ It has been tried to introduce oxygen functional groups by the harsh acids oxidation to increase the binding sites.⁵ However, the conventional chemical treated catalysts are always show poor performance in catalytic reactions, which is caused by the structure damage (and thus lead to decrease in the conductivity of CNTs).⁶ Recently, the low temperature plasma, reported as a green and mild surface functional approach, shows a huge potential in the surface modification. The functional groups can be effectively introduced to the CNTs surface without using chemicals, while structural destruction to CNTs is avoided.^{7,8} The low temperature plasma is also used to prepare the metal catalysts because of its non-equilibrium property, low power requirement, and the capacity to induce physical and chemical reactions for the reduction of metal precursors at relatively low temperature.⁹ According to the reports, several active catalysts are obtained by using low temperature plasma.¹⁰ More importantly, the well dispersed nanoparticles can be achieved without using any chemical reductants.¹¹ Accordingly, the low temperature plasma is a promising approach for both CNTs modification and Pt reduction, which is a mild, green, simple and highly efficient method for catalysts preparation.

The CNTs used in this work are O₂ plasma treated. These O₂ plasma treated CNTs (O₂-CNTs) are terminated with the COOH, C-OH and C=O functional groups et al. (see in Figure 1a), which endow them with a hydrophilic surface to anchor the metal precursors.¹² After the O₂-CNTs impregnated with the Pt precursors and dried in the N₂ flow, two different plasma were used to reduce the composites (the detailed experimental section see in ESI†). The Ar plasma treated catalysts is denoted as Pt/CNTs-A, and the H₂ plasma treated catalysts is denoted as Pt/CNTs-H. For comparison, catalysts prepared by the impregnation-precipitation method using NaBH₄ as reductant is denoted as Pt/CNTs-C. The representative images of Pt/CNTs-A and Pt/CNTs-H (Figure 1b and 1c) demonstrate that Pt nanoparticles are deposited on the CNTs surface without any obvious agglomerations. The uniform distributions of Pt nanoparticles with diameters around 1.77 nm and 1.49 nm are observed for Pt/CNTs-A and Pt/CNTs-H. On the other hand, Pt nanoparticles of Pt/CNTs-C are distributed inhomogeneously, which is due to the poor selectivity of chemicals (Fig. 1d). The uniform dispersions of particles in plasma reduced catalysts can be ascribed to the property of plasma discharge. We consider that the electrons in plasma are trapped on the same metal particles, and the strong coulomb repulsion is therefore elongated or distorted the bonds of it, so the particles are easily split if collided by other energetic species.

Figure 2 is the X-ray diffraction (XRD) patterns of Pt/CNTs-A, Pt/CNTs-H and Pt/CNTs-C. The diffraction peaks at 26.1° and 53.9° are assigned to the graphite crystallographic planes (002) and (004) of CNTs. We notice that the C (002) peak of Pt/CNTs-C at 26.1° is broadened, because of the decreased delocalization of the carbon system,¹³ which may be caused by the destruction of CNTs structure (Fig. 1d). The significant peaks at 39.7°, 46.2° and 67.5° are assigned to Pt (111), Pt (200) and Pt (220), respectively. This result indicates that Pt nanoparticles deposited on CNTs as a form of face-centered cubical (fcc) structure, and strongly suggests that low temperature plasma is capable of reducing metal precursors. The mechanism of low temperature plasma in reducing the precursors probably involves two processes.¹⁴ First, the high energy species such as electrons, ions and radicals are generated by plasma discharge. The second is that Pt precursors directly contact with these species through a recombination process and to be reduced. According to the research published by Lee et al.,¹⁵ the electrons are the strong reducer in plasma discharge, and the Pt ions (PtCl₆²⁻) can be reduced through the reaction below:



The electro-catalytic activities of Pt/CNTs-A, Pt/CNTs-H and Pt/CNTs-C with carbon paper for electrodes are examined. Figure 3a displays the cyclic voltammograms (CVs) curves of the electrodes measured in the nitrogen purged 1.0 M H₂SO₄ solutions. The current are normalized by the Pt loading (see in ESI†). The Electrochemical Surface Area (ECSA) of Pt nanoparticles on CNTs supports can be estimated by using the following equation from the area of H-desorption peak:¹⁶

$$S_{\text{ECSA}} = \frac{Q_{\text{H}}}{0.21 \times L_{\text{Pt}}} \quad [2]$$

where S_{ECSA} represents the ECSA (cm² mg⁻¹), Q_{H} (mC cm⁻²) is the charge transfer during the electro-desorption of H₂ on Pt sites, and the L_{Pt} (mg m⁻²) is Pt loading on electrodes, 0.21 (mC m⁻²) is the charge required to oxidize a monolayer of H₂ on smooth Pt. As shown in Table I, the ECSA of Pt/CNTs composites decrease by the following order: Pt/CNTs-H (137.9 m² g⁻¹) > Pt/CNTs-A (90.1 m² g⁻¹) > Pt/CNTs-C (36.9 m² g⁻¹). It can be seen that Pt/CNTs-H has a much larger ECSA compared to Pt/CNTs-A, which is due to the smaller particle size. Higher active surface area of plasma reduced catalysts than Pt/CNTs-C and the commercial E-TEK catalysts can be attribute to the well dispersed Pt nanoparticles.¹⁷

Table I. Electrochemical active surface area and methanol electro-oxidation activities of the Pt/CNTs-A, Pt/CNTs-H and Pt/CNTs-C.

Sample	S_{ECSA} (m ² g ⁻¹)	Forward peak current density (mA mg ⁻¹ Pt)	I _F /I _R ratio
Pt/CNTs-A	90.1	92.7	1.62
Pt/CNTs-H	137.9	213.2	4.85
Pt/CNTs-C	36.9	58.0	4.61

²E-mail: smmusc@mail.ustc.edu.cn

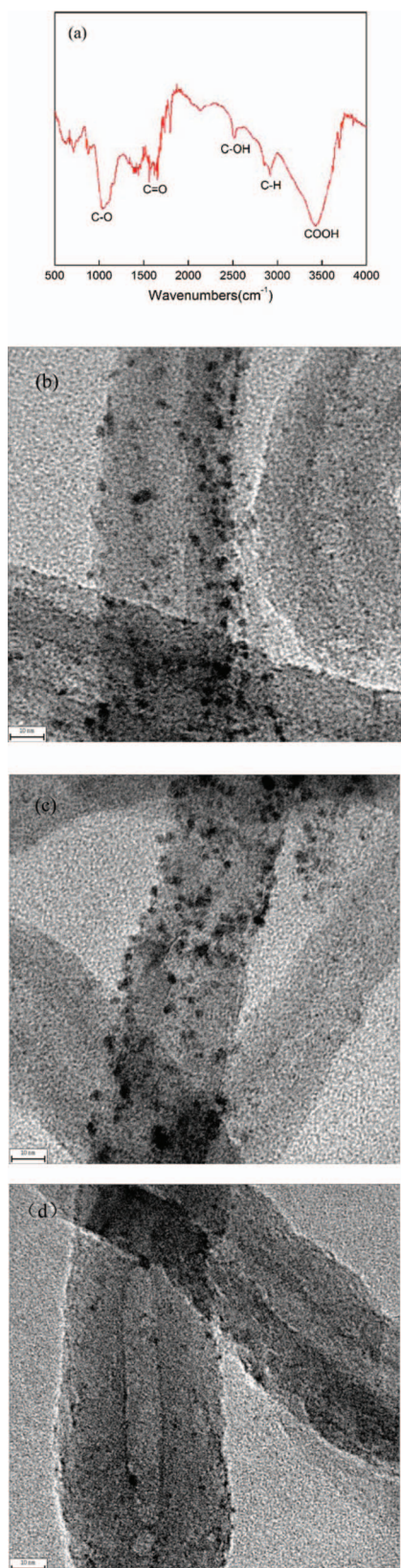


Figure 1. (a) Is the IR spectra of O₂-CNTs; (b), (c) and (d) are the TEM images of Pt/CNTs-A, Pt/CNTs-H and Pt/CNTs-C, respectively.

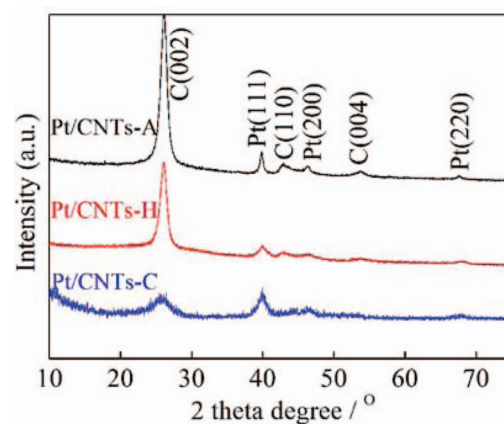


Figure 2. Is the XRD patterns of Pt/CNTs-A, Pt/CNTs-H and Pt/CNTs-C.

The electro-oxidation of methanol is characterized by CVs in the nitrogen purged 0.5 M H₂SO₄ and 1.0 M CH₃OH solutions. Two separated anodic peaks in forward (I_F) and reverse scans (I_R) are observed, and the well-known features of methanol oxidation are presented in Figure 3b. The magnitude of the peak current density in forward scan corresponds to the catalytic activity of the Pt-based catalysts for the methanol oxidation reaction. Higher current density indicates catalysts have a better performance in methanol electro-oxidation at the electrodes. As can be seen in Table I, the current density decreases by

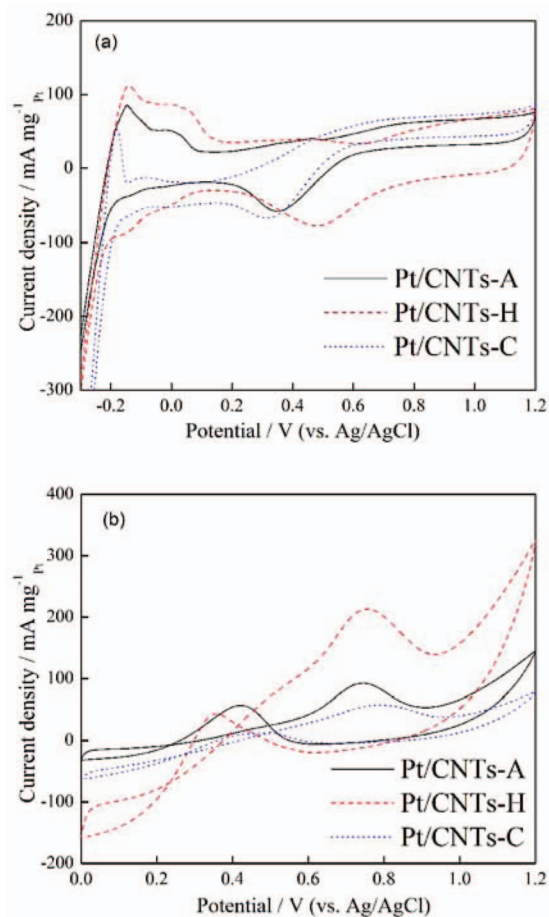
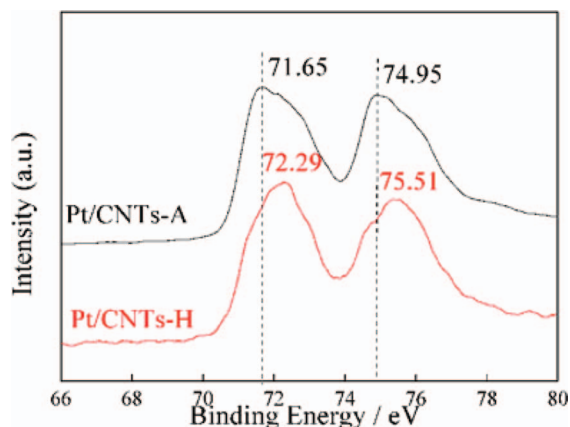


Figure 3. Cyclic voltammograms of Pt/CNTs-A, Pt/CNTs-H and Pt/CNTs-C in 1.0 M H₂SO₄ solutions (a), and 0.5 M H₂SO₄ + 1.0 M CH₃OH solutions (b) taken at a sweep rate of 50 mV s⁻¹.

Table II. C and O compositions of Pt/CNTs-A, Pt/CNTs-H and O₂-CNTs from XPS spectrums.

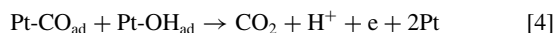
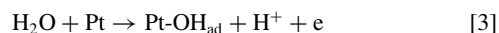
Sample	Element composition (At.%)		Atomic ratio C/O
	C	O	
Pt/CNTs-A	91.99	6.45	14.26
Pt/CNTs-H	94.14	4.54	20.74
O ₂ -CNTs	93.05	6.95	13.38

the following order: Pt/CNTs-H (213.2 mA mg⁻¹ Pt) > Pt/CNTs-A (92.7 mA mg⁻¹ Pt) > Pt/CNTs-C (58.0 mA mg⁻¹ Pt). We notice that Pt/CNTs-H has a much higher peak current density compare to other catalysts. This can be ascribed to the well dispersed nanoparticles of Pt/CNTs-H. It is also worth noting that the peak current density of Pt/CNTs-H is increased 130%, although its ECSA is only increased 53%, compared to Pt/CNTs-A. Since the current density is produced by each Pt nanoparticles, and two samples have almost the same Pt loadings and particle sizes, it is reasonable to assume that the three dimensional structures between Pt nanoparticles and CNTs supports are different (and thus lead to the different transportation of electrons). We use the X-ray photoelectron spectroscopy (XPS) to verify this assumption. As shown in Table II, the hydrogen plasma is more capable of removing O species and its C versus O is 20.74, while it is 13.38 of O₂-CNTs. It may be caused by the reductive and etching abilities of H₂ plasma.¹⁸ The H· radicals reacted with O species in plasma discharge and the products are removed by the ion bombardment. According to the research published by Bittencourt et al., the formation of bonds such as Pt-O-C at the interface reduces the interaction between Pt atoms and CNTs surface,¹⁹ and thus alters the electronic structure of Pt nanoparticles.²⁰ In our experiment, the removal of oxygen functional groups by H₂ plasma induces the direct contact between constituents, and causes the shift of Pt 4f_{7/2} peak to higher binding energies (Figure 4): Pt/CNTs-H (72.29 eV) > Pt/CNTs-A (71.65 eV). As a matter of fact, CNTs not only provides large surface area for the deposition of Pt nanoparticles, but also transports the oxidation electrons from Pt nanoparticles to external circuit to complete a cell cycle. According to the research published by Jiang et al.,⁷ the electrons can cross the interface more easier with fewer impurities between Pt nanoparticles and CNTs supports. Although the functional groups such as C=O, C-OH and COOH act as anchoring

**Figure 4.** Is the high resolution Pt4f spectrums of Pt/CNTs-A and Pt/CNTs-H.

sites for precursors, the contact resistance between constituents are also increased. The H₂ plasma can reduce the Pt precursors and the oxygen functional groups simultaneously without any side effects. By the removal of functional groups after anchoring the precursors, higher current density is therefore obtained.

The anodic peak in the reverse scan is related to the removal of the incompletely oxidized carbonaceous species. A higher I_F/I_R value implies a better performance of catalysts in the tolerance to carbon monoxide. The reaction of CO electro-oxidation is shown below:²¹



As we know, the decreased interface resistance between Pt nanoparticles and CNTs supports accelerates the transfer of the electrons,²² therefore, increases the oxidation rate of carbon monoxide, and leads to the excellent anti-poisoning property of Pt/CNTs-H.

Herein, we use the low temperature plasma discharge to modify the CNTs surface with the oxygen functional groups and reduce the anchored Pt precursors, which demonstrates that plasma is a green, mild and highly efficient method for the catalysts preparation. It is also demonstrated that H₂ plasma is capable of reducing Pt precursors and oxygen functional groups simultaneously with well nanoparticles dispersion, and the reduced contact resistance improved the catalytic activity in the methanol electro-oxidation and enhanced the tolerance of catalysts to carbonaceous species.

Acknowledgments

The project is financially supported by the Chinese National Natural Science Foundation (No. 10975162) and the Institute of Plasma Physics, Chinese Academy of Sciences (No. 095GZ1156Y).

References

1. T. R. Ralph and M. P. Hogarth, *Platinum Metals. Rev.*, **46**, 3 (2002); H. J. Huang, D. P. Sun, and X. Wang, *J. Phys. Chem. C*, **115**, 39 (2011).
2. G. N. Vayssilov, Y. Lykhach, A. Migani, T. Staudt, G. P. Petrova, N. Tsud, T. Skala, A. Bruix, F. Illas, K. C. Prince, V. Matolin, K. M. Neyman, and K. M. Libuda, *J. Nat. Mater.*, **10**, 4 (2011).
3. X. R. Ye, Y. H. Lin, and C. M. Wai, *Chem. Commun.*, **5**, 642 (2003).
4. K. Balasubramanian and M. Burghard, *Small*, **1**, 2 (2005).
5. N. Rajalakshmi, H. Ryu, M. M. Shaijumon, and S. Ramaprabhu, *J. Power Sources*, **140**, 2 (2005); W. Li, C. Liang, W. Zhou, J. Qiu, Z. Zhou, G. Sun, and Q. Xin, *J. Phys. Chem. B*, **107**, 26 (2003).
6. J. Zhang, J. H. Yang, R. P. Jia, X. Wang, and J. Huang, *New Carbon Mater.*, **25**, 4 (2010).
7. Z. Q. Jiang, X. Y. Yu, Z. J. Jiang, Y. D. Meng, and Y. C. Shi, *J. Mater. Chem.*, **19**, 37 (2009).
8. Z. Q. Jiang, Z. J. Jiang, and Y. D. Meng, *Appl. Surf. Sci.*, **257**, 7 (2011).
9. C. J. Liu, G. P. Vissokov, and B. Jang, *Catal. Today*, **72**, 173 (2002).
10. Z. Wang and Ralph T. Yang, *J. Phys. Chem. C*, **114**, 13 (2010).
11. C. J. Liu, J. J. Zou, K. L. Yu, D. G. Cheng, Y. Han, J. Zhan, C. Ratanatawanate, and B. W. L. Jang, *Pure. Appl. Chem.*, **78**, 6 (2006).
12. W. K. Oh, H. Yoon, and J. Jang, *Diam. Relat. Mater.*, **18**, 10 (2009).
13. D. Q. Yang and E. Sacher, *Chem. Mater.*, **18**, 7 (2006).
14. Z. J. Wang, Y. Zhao, L. Cui, H. Y. Du, P. Yao, and C. J. Liu, *Green Chem.*, **9**, 6 (2007).
15. S. W. Lee, D. Liang, X. P. A. Gao, and R. M. Sankaran, *Adv. Funct. Mater.*, **21**, 11 (2011).
16. X. Y. Zhang, W. Lu, J. Y. Da, H. T. Wang, D. Y. Zhao, and P. A. Webley, *Chem. Commun.*, **2**, 195 (2009).
17. M. S. Saha, R. Y. Li, and X. L. Sun, *J. Power Sources*, **177**, 2 (2008).
18. G. Y. Zhang, P. F. Qi, X. R. Wang, Y. R. Lu, D. Mann, X. I. Li, and H. J. Dai, *J. Am. Chem. Soc.*, **128**, 18 (2006).
19. C. Bittencourt, M. Hecq, A. Felten, J. J. Pireaux, J. Ghijsen, M. P. Felicissimo, P. Rudolf, W. Drube, X. Ke, and G. Van Tendeloo, *Chem. Phys. Lett.*, **462**, 4 (2008).
20. S. G. Chen, Z. D. Wei, L. Guo, W. Ding, L. C. Dong, P. K. Shen, X. Q. Qi, and L. Li, *Chem. Commun.*, **47**, 39 (2011).
21. F. Maillard, M. Eikerling, O. V. Cherstikov, S. Schreier, E. Savinova, and U. Stimming, *Faraday Discuss.*, **125**, 357 (2004).
22. S. Y. Wang, S. P. Jiang, T. J. White, J. Guo, and X. Wang, *J. Phys. Chem. C*, **113**, 43 (2009).